

Spectroscopy of the Electron-Electron Interaction in Solids

N. Fominykh, J. Berakdar,* J. Henk, and P. Bruno

Max-Planck Institut für Mikrostrukturphysik, Weinberg 2, 06120 Halle, Germany

(Received 26 March 2002; published 2 August 2002)

The spectrum of a photoexcited electron pair carries detailed information on the electron-electron interaction in metals. This is deduced from the results of a theoretical model presented here for the treatment of the double-photoelectron emission from surfaces. Main features in the two-particle spectra are assigned to (a) the exchange-correlation interaction, (b) the electronic band structure, (c) the photoelectron diffraction, and (d) the specific experimental setup. Comparison with experiments is made and common features and differences to the atomic case are pointed out.

DOI: 10.1103/PhysRevLett.89.086402

PACS numbers: 71.20.-b, 32.80.Rm, 33.55.Ad, 79.20.Kz

In recent years, angular and spin-resolved ultraviolet (UV) single-photoelectron spectroscopy [1] has witnessed an impressive refinement in resolution, allowing for a yet more detailed study of material properties. Currently this technique is intensively applied to unravel features governed by many-body effects, such as superconductivity [2,3], correlated excitations in low-dimensional systems [4–6], and the influence of electronic correlation on the spectrum [7,8]. Single-particle techniques have, however, a principle limitation in exposing the details of electronic correlation: An external perturbation introduced to probe the sample may excite simultaneously many degrees of freedom of the specimen; e.g., interacting electrons share the energy of a UV photon and the compound as a whole is then excited. Resolving the excited state of *one* of the electrons, as in single-photoelectron emission (SPE), yields integral information on the influence of the coupling to the surrounding medium. Obviously, more details are revealed on how and whether the particles are interacting if the states of *two* photoexcited particles are measured. For example, the *double*-photoelectron emission (DPE) is forbidden in the absence of correlation [9]; in case the DPE reaction may take place, the measured two-particle spectra provide direct insight into the energy and the angular dependence of the pair-correlation functions (cf. below).

In atomic and molecular physics, this kind of correlation spectroscopy has recently been realized and is currently under intensive experimental and theoretical research (cf. [10–12] for earlier references). While electronic correlation has some striking manifestations in solids [13], it is only recently that fully resolved DPE measurements from surfaces have been conducted [14]. The main experimental obstacle in this case are the low-counting coincidence rates of two *correlated* electrons as compared to the large amount of (background) uncorrelated secondary electrons. With the development of a new generation of detectors [15], it is, however, conceivable that the DPE technique for solids will undergo major advances in the near future.

On the theoretical side, an adequate treatment of electronic correlation, in particular, of the interaction between the photoexcited electron pair, is a prerequisite for the description of DPE [9,16,17]. An important step in this

direction is the recent development of a version of the density-functional theory (DFT) that describes the ground state in terms of correlated many-particle densities [18,19]. For the calculation of DPE spectra, one needs, however, in addition to the correlated ground state, an expression for the correlated two-particle state.

This Letter provides the first theory for DPE from solids with a realistic *ab initio* calculation of the (single-particle) electronic structure of the sample. Correlated two-particle states are generated upon the coupling of two single-particle states via a model potential of the screened Coulomb type. The goals of this work are (i) the calculation of both SPE and DPE spectra within the same approach to contrast conclusively the information obtained from both techniques and to assess the reliability of the single-particle part of the DPE theory, (ii) the analysis of how the electron-electron interaction manifests itself in the DPE spectra, (iii) the study of the DPE surface sensitivity (compared to SPE) and of the dependence of DPE on the photoelectron energies and emission angles, (iv) the comparison of theory with available experiments, and (v) the analysis of differences and similarities to DPE from single atoms.

Theory.—Within the one-step model of SPE, the current $J^{(1)}$ [20] of photoelectrons emitted with a surface-parallel wave vector \mathbf{k}_{\parallel} and an energy ϵ , upon the absorption of a UV photon with energy ω , is given by

$$J^{(1)} \propto -\text{Im}\langle\Psi^{(1)}|\Delta g^r(\epsilon - \omega)\Delta^\dagger|\Psi^{(1)}\rangle. \quad (1)$$

The final state $|\Psi^{(1)}\rangle = g^a|\mathbf{k}_{\parallel}, \epsilon\rangle$ is obtained by propagating (back) the detector state $|\mathbf{k}_{\parallel}, \epsilon\rangle$ using the advanced Green function g^a . The photohole state is described by the retarded Green function g^r , and Δ is the dipole operator of the incident radiation. In the one-step DPE process, one photon ejects *two* electrons with wave vectors $\mathbf{k}_{1\parallel}$ and $\mathbf{k}_{2\parallel}$ and energies E_1 and E_2 from the occupied states of a metal surface. The double-photoelectron current $J^{(2)}$ can be approximated by [16]

$$J^{(2)} \propto \int_{E_{\min}}^{E_{\text{F}}} \langle\Psi^{(2)}|\Delta \text{Im}g^r(\epsilon) \text{Im}g^r(E - \omega - \epsilon)\Delta^\dagger|\Psi^{(2)}\rangle d\epsilon, \quad (2)$$

where E_F is the Fermi energy, $E = E_1 + E_2$, and $E_{\min} = E - \omega - E_F$. The correlated two-particle final state $|\Psi^{(2)}\rangle = G^a|k_{1\parallel}, E_1; k_{2\parallel}, E_2\rangle$ is obtained from the uncorrelated detector states $|k_{1\parallel}, E_1; k_{2\parallel}, E_2\rangle = |k_{1\parallel}, E_1\rangle \otimes |k_{2\parallel}, E_2\rangle$ via the two-particle Green function G^a . The occupied nonlocal density related to electron j is determined by $\text{Im}g^r(k_{j\parallel}, \epsilon_j)$, $j = 1, 2$.

To elucidate the features of DPE as compared to SPE, we employ a calculational scheme for the currents $J^{(1)}$ and $J^{(2)}$ in which the single-particle states are evaluated simultaneously. The ground-state single-particle electronic structure is obtained from an *ab initio* linear muffin-tin orbital method based on the local density approximation of DFT. For the photoemission calculations, we utilize the layer Korringa-Kohn-Rostoker (LKKR) method [21].

The explicit incorporation of the mutual interaction U between the two excited photoelectrons is indispensable for an adequate description of DPE [9]. Here, this is achieved as follows: For a nearly free electron metal, U is screened with a screening length λ dependent on the density of states $N(E_F)$ [$\lambda = 1/\sqrt{4\pi N(E_F)}$; for Cu, $\lambda \approx 2.66$ Bohr]. In the long-wavelength limit, U depends only on the coordinate difference $\mathbf{r}_1 - \mathbf{r}_2$, namely, $U(\mathbf{r}_1, \mathbf{r}_2) = e^{(-|\mathbf{r}_1 - \mathbf{r}_2|/\lambda)}/|\mathbf{r}_1 - \mathbf{r}_2|$. To determine the two-particle state $|\Psi^{(2)}\rangle$, we first employ the LKKR method and obtain the single-particle states $|\psi_j(\mathbf{k}_j)\rangle = g^r|k_{j\parallel}, \epsilon_j\rangle$, $j = 1, 2$. Using the procedure developed in [22], $|\psi_1(\mathbf{k}_1)\rangle$ and $|\psi_2(\mathbf{k}_2)\rangle$ are then coupled to each other via U to determine the state $|\Psi^{(2)}\rangle$ [and subsequently the current $J^{(2)}$, Eq. (2)]. In this way, single-particle and two-particle photocurrents are calculated within the same scheme allowing a sensible comparison. From the functional form of U , it is clear that $J^{(2)}$ depends not only on the energies and emission directions of the photoelectrons, as in the SPE case, but also on the mutual angle between the photoelectrons: If the electrons are close to each other, U provides a strong coupling, whereas U (and, hence, the DPE signal [9]) is strongly suppressed when the photoelectrons are separated at distances larger than λ . This general statement is quantified below by numerical results.

Reliability of the SPE part.—Figure 1(a) shows a measured angular distribution of the SPE intensity from Cu(001) [23]. Our calculations for $J^{(1)}$ [Fig. 1(b)] agrees with the experiments which indicates an adequate treatment of the single-particle part of the problem.

Symmetry of the angular distribution.—The SPE angular distributions reflect the $4mm$ symmetry of the Cu(001) surface [Figs. 1(a) and 1(b)]. In contrast, the presence of a second photoelectron in DPE dictates a different symmetry of the angular distribution. In Figs. 1(c) and 1(d), the DPE current is depicted as a function of k_{\parallel} of one electron, while k_{\parallel} of the other electron is fixed. If this “fixed” electron is detected in off-normal emission, the symmetry is reduced [to m in Fig. 1(d)]. However, if the fixed electron is detected with $k_{\parallel} = 0$, the distributions of DPE and SPE show the same symmetry [$4mm$ in Fig. 1(c)].

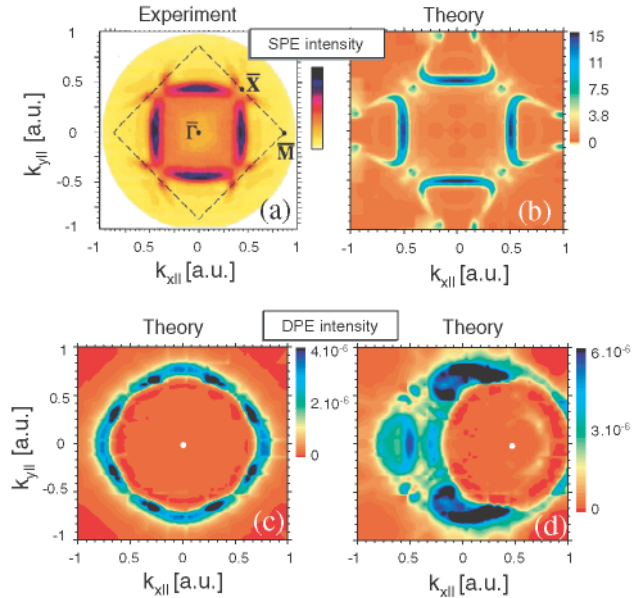


FIG. 1 (color online). Angular distribution of photoemission from the Fermi level of Cu(001). (a) Experimental single-photoelectron emission (SPE) intensity vs surface-parallel wave vector $\mathbf{k}_{\parallel} = (k_{x\parallel}, k_{y\parallel})$. The photon energy of the unpolarized light is $\omega = 21.2$ eV. (b) Theoretical results corresponding to case (a) with light incident normally to the surface. (c) and (d) Double-photoemission (DPE) intensities for photoelectrons having equal energies of 16 eV and $\omega = 42.4$ eV. One electron is detected at a fixed direction marked by the white dot [at 0° (c) and 30° (d) polar angle]. The DPE intensity is then scanned as a function of k_{\parallel} of the other photoelectron.

Exchange-correlation hole.—The most notable structure in the DPE angular distributions is the intensity minimum centered at \mathbf{k}_{\parallel} of the fixed electron [Figs. 1(c) and 1(d)]. This “hole” is a direct manifestation of exchange and correlation between the two photoelectrons. The former is accounted for by the antisymmetry of the two-particle state, whereas the latter is mediated by the potential U . The high intensity surrounding the hole can be explained by the competition of two factors: (i) the electron-electron repulsion and the exchange interaction prevent the two electrons from escaping with comparable wave vectors within a proximity determined by the screening length. Therefore, the extent of the hole is a qualitative measure of the strength of the electron-electron interaction [for specified $(\mathbf{k}_{1\parallel}, E_1; \mathbf{k}_{2\parallel}, E_2)$]. (ii) If the two electrons are well separated from each other, the electron-electron interaction U becomes negligible and the DPE signal diminishes, for the DPE process is forbidden in the absence of U [9]. Combining these two effects, the distribution of the intensity around the direction of the fixed electron becomes comprehensible.

Both the shape and the extent of the correlation hole depend on the photoelectron energies: At low energies, it is large and dominates the distribution, whereas at higher

ones, it is limited to a small region [cf. Figs. 1(d) and 2(d)]. This behavior can be understood from the properties of U as reflected in the transition-matrix elements [Eq. (2)].

In those regions where the two electrons are far away from each other (U is then weak), one observes a remote reminiscence of the DPE spectra to the corresponding SPE distributions; e.g., the influence of the single-electron diffraction is observable, slightly distorted due to the presence of the second (fixed) electron (Fig. 2).

Surface sensitivity.—Since two electrons have to escape the surface, DPE is expected to be more surface sensitive than SPE. In a crude model, the escape probability p for a single electron decays exponentially with the distance from the surface, $p \sim \exp(-z/\ell)$, where ℓ is the escape depth. The escape probability for two electrons is then $\exp(-2z/\ell)$; i.e., the escape depth is effectively halved. Hence, in SPE theory one has to sum up contributions from deep layers (typically from the first 15 surface layers) to obtain $J^{(1)}$, as is evident from Figs. 2(a) and 2(c). In DPE, both the shape and the magnitude of the photocurrent are determined by including contributions from the first two to four surface layers [Figs. 2(b) and 2(d)].

Photoelectron diffraction.—DPE experiments from crystal surfaces reported in Refs. [14] show pronounced features in the distributions of the electron-pair total energy ($E = E_1 + E_2$) between the two electrons [Fig. 3(a)]. To uncover the origin of structures occurring in the corresponding theoretical spectra [Fig. 3(b)], it is constructive to contrast with the results of the present theory for the double photoionization of the ground state [$\text{He}(^1S^e)$] of the helium atom [Fig. 3(c)]. For the “single-site” DPE from atomic He, the cross section vanishes if $\mathbf{k}_1 + \mathbf{k}_2$ is perpendicular to

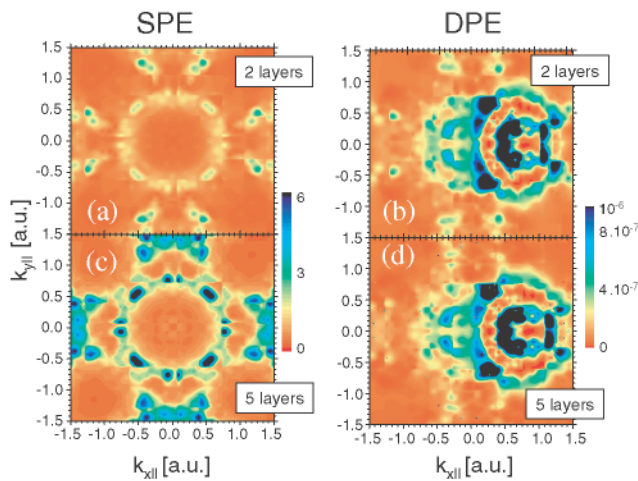


FIG. 2 (color online). Surface sensitivity of SPE [(a) and (c)] and DPE [(b) and (d)] from Cu(001). The setups are chosen as in Figs. 1(b) and 1(d), respectively, but the photoelectron energies are increased to 36 eV. The photon energy is 41 eV for SPE and 82 eV for DPE. In (a) and (b) [(c) and (d)] the contributions to the photocurrent from the two (five) outermost surface layers are depicted.

the polarization vector of the incoming photon [12], which occurs in Fig. 3(c) at $E_1 = E_2$. This propensity rule holds for solids, too, but in the absence of photoelectron diffraction [9]. Indeed, we argue here that the photoelectron diffraction is the reason for the finite photocurrent $J^{(2)}$ at $E_1 = E_2$ found for Ni(001) in Figs. 3(a) and 3(b): For a periodic surface, the electronic states are eigenstates of the lattice translations; i.e., they can be expanded into plane waves. Hence, the effect of the lattice can be investigated by varying the number n of plane waves included in the expansion of the photoelectron states. The inset of Fig. 3(b) shows the DPE current for $E_1 = E_2$ and $\theta_1 = \theta_2$ vs n . Indeed, $J^{(2)}$ decreases rapidly with decreasing n and saturates at about $n \approx 20$. This behavior corroborates both the propensity rule and the explanation of the finite DPE photocurrent at $E_1 = E_2$.

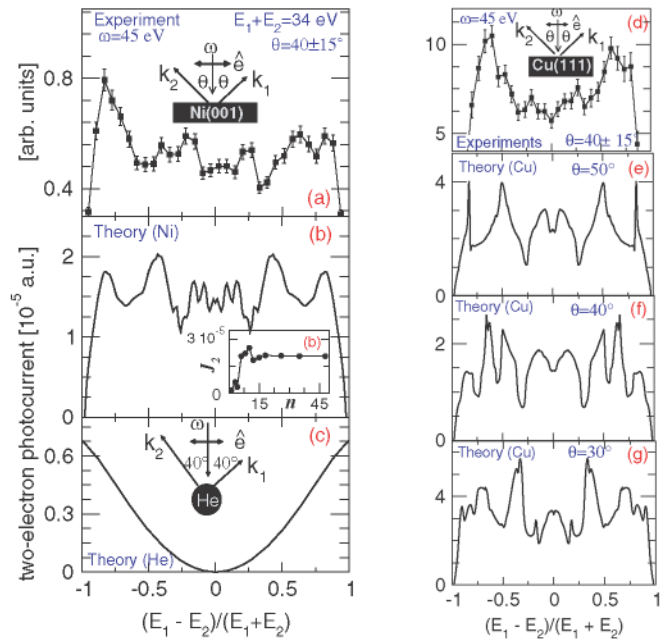


FIG. 3 (color online). (a) Experimental DPE intensity from Ni(001) [14]. The wave vectors \mathbf{k}_1 and \mathbf{k}_2 of the emitted electrons and the linear polarization vector of the light $\hat{\mathbf{e}}$ are coplanar (cf. inset). The total energy of the electron-pair is fixed as $E = E_1 + E_2 = 34 \pm 1$ eV with $\omega = 45$ eV. The DPE current is scanned as a function of the energy sharing $(E_1 - E_2)/E$. The electron detectors are fixed at symmetric positions (40° polar angle) and have an angular resolution of $\pm 15^\circ$. (b) Theoretical results corresponding to case (a), with account for the experimental angular resolution. Inset: DPE current $J^{(2)}$ (at $E_1 = E_2$) vs number n of plane waves included in the expansion of the photoelectron wave. (c) As in (b), but for a single He atom in state $^1S^e$; ω is adjusted to compensate for the double ionization threshold of He. For the ground state the two-electron wave function of Ref. [24] is employed. (d) As in (a), but for Cu(111). (e)–(g) Theoretical results corresponding to (d) but with varying escape angles $\theta_1 = \theta_2$ [$\theta = 50^\circ$ (e), $\theta = 40^\circ$ (f), $\theta = 30^\circ$ (g)].

Density-of-states effect.—Assuming parabolic dispersion of the photoelectron states in the vacuum (which means $dE_j = k_j dk_j$; $j = 1, 2$), one obtains for the fully resolved DPE current in spherical coordinates $J^{(2)}(\theta_1, \varphi_1, E_1; \theta_2, \varphi_2, E_2) = CJ^{(2)}(\mathbf{k}_1, \mathbf{k}_2)$, where $C = k_1 k_2$, and φ_1 as well as φ_2 are azimuthal angles [9,12]. In the atomic case, the density of states (DOS) for one photoelectron in the field of the residual ion behaves as $1/k_j$ for $k_j \rightarrow 0$ (and $k_i \gg k_j$) [25]; i.e., for one electron the DOS diverges at the ionization threshold. This DOS effect combined with the kinematical factor $C = k_1 k_2$ leads, in general, to a finite DPE current from atoms when the energy of one of the electrons diminishes. In contrast, for surfaces, the DOS is finite at the vacuum level ($k_j \approx 0$) and, hence, the DPE current [$k_1 k_2 J^{(2)}(\mathbf{k}_1, \mathbf{k}_2)$] vanishes if E_1 or E_2 is very small. This profound difference between atoms and solids is confirmed by our calculations: In contrast to DPE from surfaces (Fig. 3), for He($1S^e$) the DPE current is finite for $E_1 \rightarrow 0$ or $E_2 \rightarrow 0$ [Fig. 3(c)].

Band-structure effect.—In Fig. 3, both the photon energy ω and the electron-pair energy $E = E_1 + E_2$ are fixed. This specifies the initial binding energy of the electron pair as $\epsilon = \omega - E$. For atoms, ϵ pins down the initial state to a specific, discrete level. For surfaces, the electronic structure is dependent not only on the energy ϵ_i , but also on the Bloch wave vectors $\mathbf{q}_{i\parallel}$. When varying $(E_1 - E_2)/E$ (for fixed E , ω , and hence fixed ϵ), one scans through different $\mathbf{k}_{i\parallel}$ [Figs. 3(e)–3(g)]. Therefore, the relevant $\mathbf{q}_{i\parallel}$ and the associated electronic levels appear as sharp peaks in $J^{(2)}$ at certain $(E_1 - E_2)/E$ [16]. A similar effect arises due to the energy integration in Eq. (2) which involves several single-particle levels. In consequence, the structure of the initial-state spectral density is reflected as pronounced maxima and minima in the DPE spectra. In contrast, the smooth spectral density of the jellium model results in smooth DPE spectra [9].

Concerning the comparison with experiments, it should be remarked that the shape of the DPE spectrum changes substantially within the experimental angular resolution [Figs. 3(e)–3(g)]. This is due to the fact that, with increasing polar angles, the allowed range for the initial $\mathbf{k}_{i\parallel}$ is stretched and different initial states contribute to the photocurrent. For $\theta \rightarrow 0$, the DPE current vanishes at $E_1 = E_2$ due to the electron-electron repulsion, whereas for $\theta \rightarrow \pi/2$, it decreases due to the weakening of the electron-electron interaction [cf. also Figs. 1(c) and 1(d)].

In conclusion, we present pilot results to highlight the general aspects and the power of DPE from surfaces as a novel tool for electronic-correlation imaging.

We thank J. Kirschner, S. Samarin, A. Morozov, R. Dörner, M. Hattas, G. Stefani, R. Gotter, A. Ernst, R. Feder, and H. Gollisch for enlightening discussions.

*Electronic address: jber@mpi-halle.de

- [1] S. Hüfner, *Photoelectron Spectroscopy* (Springer, New York, 1995).
- [2] A. Lanzara *et al.*, *Nature (London)* **412**, 510 (2001).
- [3] T. Yokoya *et al.*, *Science* **294**, 2518 (2001).
- [4] Y. D. Chuang *et al.*, *Science* **292**, 1509 (2001).
- [5] P. Segovia *et al.*, *Nature (London)* **402**, 504 (1999).
- [6] S. Maekawa *et al.*, *Rep. Prog. Phys.* **64**, 383 (2001).
- [7] A. Marini *et al.*, *Phys. Rev. Lett.* **88**, 016403 (2002).
- [8] L. Hedin, *J. Phys. Condens. Matter* **11**, R489 (1999).
- [9] J. Berakdar, *Phys. Rev. B* **58**, 9808 (1998).
- [10] P. Selles *et al.*, *Phys. Rev. A* **65**, 032711 (2002); A. S. Kheifets and I. Bray, *ibid.* **65**, 012710 (2002); S. Senz and N. Chandra, *ibid.* **65**, 052702 (2000); A. Knapp *et al.*, *Phys. Rev. Lett.* **89**, 033004 (2002); J. Colgan *et al.*, *J. Phys. B* **34**, L457 (2001); M. Walter *et al.*, *ibid.* **33**, 2907 (2000).
- [11] J. B. West *et al.*, *J. Phys. B* **34**, 4169 (2001); C. Dawson *et al.*, *ibid.* **34**, L525 (2001); P. Bolognesi, *ibid.* **34**, 3193 (2001); M. Achler *et al.*, *ibid.* **34**, 965 (2001); T. Masuoka, *J. Chem. Phys.* **115**, 264 (2001); S. A. Collins *et al.*, *Phys. Rev. A* **64**, 062706 (2001); S. Rioual *et al.*, *Phys. Rev. Lett.* **86**, 1470 (2001); A. Huetz *et al.*, *ibid.* **85**, 530 (2000).
- [12] J. S. Briggs and V. Schmidt, *J. Phys. B* **33**, R1 (2000); G. C. King and L. Avaldi, *ibid.* **33**, R215 (2000); J. Berakdar and H. Klar, *Phys. Rep.* **340**, 473 (2001).
- [13] P. Fulde, *Electron Correlation in Molecules and Solids* (Springer, Berlin, 1991).
- [14] R. Herrmann *et al.*, *Phys. Rev. Lett.* **81**, 2148 (1998); *J. Phys. IV (France)* **9**, 127 (1999); H. W. Biester *et al.*, *Phys. Rev. Lett.* **59**, 1277 (1987).
- [15] J. Kirschner and M. Hattas (private communication).
- [16] N. Fominykh *et al.*, *Solid State Commun.* **113**, 665 (2000).
- [17] N. Fominykh *et al.*, in *Correlations, Polarization and Ionization in Atomic Systems*, AIP Conf. Proc. No. 604 (AIP, New York, 2002), p. 210.
- [18] A. Gonis *et al.*, *Phys. Rev. B* **56**, 9335 (1997); *Phys. Rev. Lett.* **77**, 2981 (1996).
- [19] P. Ziesche, *Int. J. Quantum Chem.* **60**, 1361 (1996); *Phys. Rev. Lett. A* **195**, 213 (1994).
- [20] C. Caroli *et al.*, *Phys. Rev. B* **8**, 4552 (1973).
- [21] A. Gonis, *Theoretical Materials Science* (Materials Research Society, Pittsburgh, 2000).
- [22] J. Berakdar *et al.*, *Solid State Commun.* **112**, 587 (1999).
- [23] Th. Straub *et al.*, *Phys. Rev. B* **55**, 13473 (1997).
- [24] R. Bonham and D. Kohl, *J. Chem. Phys.* **45**, 2471 (1966).
- [25] J. Berakdar *et al.*, *J. Phys. B* **26**, 3891 (1993).